

Improved Flavin-Based Catalytic Photo-Oxidation of Alcohols Through Intersystem Crossing Rate Enhancement

Kirill A. Korvinson, George Nik Hargenrader, Jelena Stevanovic, Yun Xie, Jojo Joseph, Veselin Maslak, Christopher M. Hadad, and Ksenija D. Glusac

J. Phys. Chem. A, **Just Accepted Manuscript** • DOI: 10.1021/acs.jpca.6b08405 • Publication Date (Web): 26 Aug 2016

Downloaded from <http://pubs.acs.org> on August 31, 2016

Just Accepted

“Just Accepted” manuscripts have been peer-reviewed and accepted for publication. They are posted online prior to technical editing, formatting for publication and author proofing. The American Chemical Society provides “Just Accepted” as a free service to the research community to expedite the dissemination of scientific material as soon as possible after acceptance. “Just Accepted” manuscripts appear in full in PDF format accompanied by an HTML abstract. “Just Accepted” manuscripts have been fully peer reviewed, but should not be considered the official version of record. They are accessible to all readers and citable by the Digital Object Identifier (DOI®). “Just Accepted” is an optional service offered to authors. Therefore, the “Just Accepted” Web site may not include all articles that will be published in the journal. After a manuscript is technically edited and formatted, it will be removed from the “Just Accepted” Web site and published as an ASAP article. Note that technical editing may introduce minor changes to the manuscript text and/or graphics which could affect content, and all legal disclaimers and ethical guidelines that apply to the journal pertain. ACS cannot be held responsible for errors or consequences arising from the use of information contained in these “Just Accepted” manuscripts.



1
2
3
4
5
6
7
8
9
10
11
12
13
14
15
16
17
18
19
20
21
22
23
24
25
26
27
28
29
30
31
32
33
34
35
36
37
38
39
40
41
42
43
44
45
46
47
48
49
50
51
52
53
54
55
56
57
58
59
60

Improved Flavin-based Catalytic Photo-oxidation of Alcohols Through Intersystem Crossing Rate Enhancement

*Kirill A. Korvinson,[†] George N. Hargenrader,[†] Jelena Stevanovic,[§] Yun Xie,[†] Jojo Joseph,[‡]
Veselin Maslak,[§] Christopher M. Hadad[‡] and Ksenija D. Glusac^{**†}*

[†]Department of Chemistry, Center for Photochemical Sciences, Bowling Green State University,
Bowling Green, Ohio 43403, United States

[‡]Department of Chemistry and Biochemistry, The Ohio State University, Columbus, OH 43210,
United States

[§]Faculty of Chemistry, University of Belgrade, Studentski Trg 12-16, Belgrade 11000, Serbia

KEYWORDS flavin, photocatalysis, organocatalysis, benzaldehyde, oxidation.

ABSTRACT

The triplet excited state formation efficiency in a flavin derivative was increased by the introduction of iodine into the molecular framework. The transient absorption measurements showed that the intersystem crossing rate was $1.1 \times 10^{10} \text{ s}^{-1}$, significantly faster than in the parent flavin compound. Furthermore, the photocatalytic efficiency of iodo-flavin was evaluated using

1
2
3 the oxidation of benzyl alcohol as a model reaction. The benzaldehyde product yields were
4 higher when iodo-flavin was used as a photocatalyst, showing that the increased triplet yield
5 directly translates into improved photocatalysis. The iodo-flavin catalyst also allowed the use of
6 higher substrate concentrations (since the undesired electron transfer from singlet excited state
7 was minimized), which is expected to improve the practical aspects of photocatalysis by flavins.
8
9
10
11
12
13
14
15

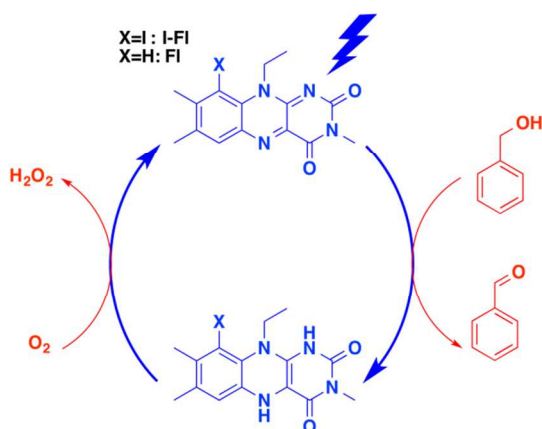
16 **Introduction**

17
18 Flavin-based monooxygenases and oxidases are exceptionally efficient in activating molecular
19 oxygen towards catalytic oxidation of a number of organic substrates.¹⁻⁶ While monooxygenases
20 insert atomic oxygen into a substrate (S) by catalyzing the reaction $S + O_2 + NADH + H^+ \rightarrow SO$
21 $+ NAD^+ + H_2O$, the oxidases perform dehydrogenation of the substrate (SH₂) by catalyzing the
22 reaction $SH_2 + O_2 \rightarrow S + H_2O_2$. Given the significance of oxidation reactions in organic
23 syntheses, the artificial biomimetic flavin-based catalysts have been extensively used to oxidize
24 organic compounds by atmospheric oxygen under mild reaction conditions.⁷ In the case of
25 oxidase-mimicking catalysts, the oxidative power of the flavin is generally enhanced by
26 photoexcitation. This photo-organocatalytic approach facilitates the oxidation of a number of
27 substrates that cannot be oxidized thermally, and has been applied towards the oxidation of
28 aromatic alcohols, amines and other substrates.⁸⁻¹⁵
29
30
31
32
33
34
35
36
37
38
39
40
41
42
43
44
45
46
47

48 Previous mechanistic studies of the photocatalytic oxidations of benzyl alcohols indicate that the
49 first step involves a photoinduced electron transfer from benzyl alcohol to the excited flavin,
50 followed by the proton and hydrogen-atom transfers to generate the oxidized benzylaldehyde
51 product and the reduced flavin FlH₂.^{16,17} The subsequent regeneration of the catalyst is achieved
52 by a reaction of FlH₂ with molecular oxygen via the flavin hydroperoxide (FlHOOH)
53
54
55
56
57
58
59
60

intermediate.¹⁸⁻²⁰ The initial photoinduced electron transfer from benzyl alcohol can occur to either singlet (S_1) or triplet (T_1) excited states of the flavin. However, a recent study by Riedle and coworkers¹⁷ reported that the electron transfer to the S_1 state is not catalytically productive, as it leads to a fast (~ 50 ps) back electron transfer. On the other hand, electron transfer to the T_1 state generates long-lived radical ions (~ 5 μ s) that undergo further proton/hydrogen-atom transfers to generate the desired product. Heavy element substituents, such as iodine, are known to increase the $S \rightarrow T$ intersystem crossing (ISC) rates in organic compounds due to spin-orbit coupling.²¹ Given the significance of triplet excited states in flavin-based photocatalysis, the aim of this study was to utilize the heavy-atom effect to increase the quantum yield for the T_1 state formation in flavins. Specifically, it will be shown that the incorporation of the iodine into the flavin framework (I-FI) leads to a significant increase in the ISC rate relative to the reference compound (FI, Scheme 1). Furthermore, this manuscript demonstrates that the increased yield of triplet formation in I-FI directly translates into improved photo-organocatalytic performance relative to the reference model compound. For this purpose, the flavin-catalyzed oxidation of benzyl alcohol to benzaldehyde was used as a model reaction (Scheme 1).

Scheme 1. General Mechanism for Organocatalytic Photooxidation of Benzyl Alcohol by Flavins.

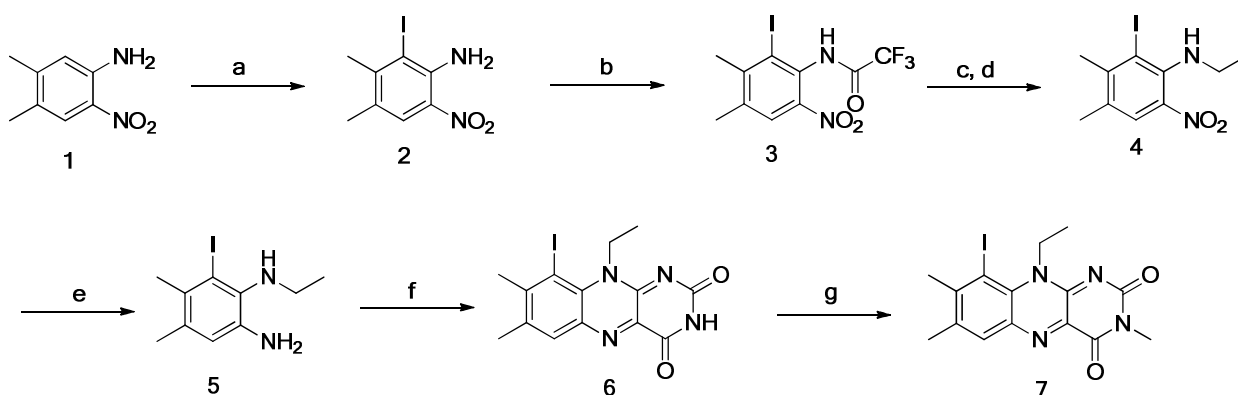


Materials and Methods

Unless specified, all reagents, starting materials and solvents (HPLC grade) were purchased from commercial sources and used as received without purification. ^1H and ^{13}C spectra were recorded at ambient temperature on Bruker Avance 300 MHz NMR or Bruker AVANCEIII 500 MHz NMR spectrometers. Spectra were described as chemical shifts (ppm), multiplicity (s, singlet; d, doublet; t, triplet; q, quartet; m, multiplet), coupling constant in hertz (Hz), and number of protons. All reactions were monitored using silica gel 60 F₂₅₄ analytical TLC plates with UV detection ($\lambda = 254$ nm and 365 nm). Silica gel (60 Å, 40-63 μm) was used as stationary phase for column chromatography.

Synthesis. The isoalloxazine structures of model flavins were synthesized using a condensation between the alloxan and the corresponding aromatic ortho-bis-amine (synthesis of Fl was reported previously).^{22,23} The synthesis of I-Fl was performed using the steps presented in Scheme 2.

Scheme 2. Synthesis of I-Fl.



a) KBrO_3 , KI , HCl , $\text{MeOH}/\text{H}_2\text{O}$, 60°C , 4h, 92%; b) TFAA, Et_3N , DCM , 4h, 82%; c) EtI , K_2CO_3 , DMF , 60°C , 26h; d) NaOH , $\text{MeOH}/\text{H}_2\text{O}$, 65°C , 3h, 76%; e) Sn , HCl , 95°C , 2h, 32%; f) alloxane monohydrate, $\text{B}(\text{OH})_3$, AcOH , 10h 67%; g) MeI , K_2CO_3 , DMF , 72h, 87%

1
2
3 **6-iodo-4,5-dimethyl-2-nitroaniline (2)** – A solution of compound **1** (15 g, 90 mmol), potassium
4 bromate (12 g, 90 mmol) and potassium iodide (15 g, 90 mmol) was prepared in 450 ml of
5 methanol/water (2:3, V:V) mixture. To the resulting solution concentrated hydrochloric acid
6 (37.5 ml, 450 mmol) was added and the mixture was heated at 60° C for 4 h. The crude product
7 was extracted with dichloromethane (3x100 ml), organic layer was washed with water, 5%
8 sodium thiosulfate, brine and dried over sodium sulfate. The solvent was removed under reduced
9 pressure and the residue was recrystallized from hexane to give 24 g (83 mmol, 80%) of 6-iodo-
10 4,5-dimethyl-2-nitroaniline as an orange solid. GCMS: m/z found 292 [291.97 calculated for
11 C₈H₉IN₂O₂]. ¹H NMR (500 MHz, CD₃CN) δ ppm: 7.95 (s, 1H), 6.74 (s, 2H), 2.43 (s, 3H), 2.30
12 (s, 3H). ¹³C NMR (500MHz, CD₃CN) δ ppm: 146.10, 141.12, 130.34, 125, 54, 124.70, 114.24,
13 20.63, 19.44.
14
15
16
17
18
19
20
21
22
23
24
25
26
27
28

29 **6-iodo-N-(4,5-dimethyl-2-nitrophenyl)-2,2,2-trifluoro-acetamide (3)** – Compound **2** (24 g, 83
30 mmol) was dissolved in 250 ml of dichloromethane. Triethylamine (9.2 ml, 6.7 g, 165 mmol)
31 and trifluoroacetic anhydride (18.5 ml, 28 g, 133 mmol) were added to the reaction mixture and
32 stirred for 4h. Solution was transferred to a separatory funnel and washed once with 150 ml of 2
33 M hydrochloric acid, three times with 100 ml portions of 2 M sodium bicarbonate and once with
34 brine. The organic fraction was dried over anhydrous calcium chloride and the excess solvent
35 was evaporated. The product was purified using flash chromatography (hexane:ethylacetate=6:1)
36 to give 28 g (72 mmol, 87%) of pure compound **3** as a white solid. GCMS: m/z found 388
37 [387.95 calculated for C₁₀H₈F₃IN₂O₃]. ¹H NMR (500 MHz, CD₃CN) δ ppm: 9.38 (s, 1H), 7.89
38 (s, 1H), 2, 50 (s, 3H), 2.45 (s, 3H). ¹³C NMR (500 MHz, CD₃CN) δ ppm: 156.7 (q, J^{C-F} = 155
39 Hz), 145.79, 141.30, 127.67, 125.98, 125.12, 21.35, 21.33.
40
41
42
43
44
45
46
47
48
49
50
51
52
53
54
55
56
57
58
59
60

1
2
3 **6-iodo-N-ethyl-N-(4,5-dimethyl-2-nitro-phenyl)-amine (4)** – Compound **3** (27 g, 70 mmol)
4
5 was dissolved in 150 ml of DMF, anhydrous potassium carbonate (19 g, 140 mmol) and 3.2 ml
6
7 of ethyl iodide (15 mL, 30 g, 190 mmol) were added and the mixture was stirred for 26 h at 60°
8
9 C. Once the conversion was completed, 100 ml of 10% solution of NaOH in methanol:water
10
11 (1:1) was added. The mixture was heated at 65° C for 3h, cooled to rt, extracted with
12
13 dichloromethane, the organic layer was dried over calcium chloride and the solvent was
14
15 evaporated under reduced pressure. The crude product was purified by flash chromatography
16
17 (hexane:ethyl acetate, 10:1) to give 16 g (50 mmol, 72%) of compound **4** as a bright orange oil,
18
19 which crystallized upon cooling. GCMS: m/z found 320 [320.00 calculated for C₁₀H₁₃IN₂O₂]. ¹H
20
21 NMR (500 MHz, CD₃CN) δ ppm: 7.67 (s, 1H), 5.54 (s, 1H), 3.13 (q, J=10 Hz, 2H), 2.41 (s, 3H),
22
23 2.29 (s, 3H), 1.15 (t, J=10 Hz, 3H). ¹³C NMR (500 MHz, CD₃CN) δ ppm: 145.41, 141.78,
24
25 129.57, 126.12, 119.67, 43.45, 21.59, 20.53, 16.09.
26
27
28
29
30

31 **6-iodo-N-ethyl-4,5-dimethyl-benzene-1,2-diamine (5)** – Compound **4** (15 g, 47 mmol) was
32
33 partially dissolved in 250 ml of 12 M HCl. The reaction mixture was heated to 95° C and tin foil
34
35 (27 g, 230 mmol) in small amounts was added to the reaction mixture until solution became
36
37 colorless. The reaction mixture was cooled down and 6 M NaOH was added drop wise until the
38
39 pH of the mixture became 10. The formed suspension was heated and passed through a bed of
40
41 celite. The filtrate was extracted with dichloromethane, the organic layer was dried over sodium
42
43 sulfate and evaporated under reduced pressure. Crude product was purified using column
44
45 chromatography (ethyl acetate:hexane 1:9) to give 4.13 g (15 mmol, 32%) of compound **5** as a
46
47 brown oil. CGMS: m/z found 290 [290.03 calculated for [C₁₀H₁₅IN₂]. ¹H NMR (500 MHz,
48
49 CD₃CN) δ ppm: 6.50 (s, 1H), 4.10 (s, 2H), 3.25 (s, 1H), 2.85 (q, J=5 Hz, 2H), 2.23 (s, 3H), 2.17
50
51
52
53
54
55
56
57
58
59
60

(s, 3H), 1.15 (t, J=7.5, 3H). ^{13}C NMR (500MHz, CD_3CN) δ ppm: 141.83, 133.93, 131.97, 125.12, 124.27, 116.68, 42.27, 21.01, 19.65, 16.06.

10-ethyl-9-iodo-7,8-dimethylbenzo[g]pteridine-2,4(3H,10H)-dione (6) – Compound **5** (3.5 g, 12.7 mmol) was added drop wise to the suspension of alloxan monohydrate (4.1 g, 25.4 mmol) and boric acid (0.4 g, 6.4 mmol) in 20 ml of glacial acetic acid. The mixture was stirred overnight and the precipitate was filtered off and recrystallized from methanol to give 3.4 g (8.5 mmol, 67%) of compound **6** as a yellow solid. MALDI MS, m/z found: 396 [396.01 calculated for $\text{C}_{14}\text{H}_{13}\text{IN}_4\text{O}_2$]. ^1H NMR (500 MHz, DMSO-d_6) δ ppm: 11.44 (s, 1H), 7.92 (s, 1H), 4.82 (q, J=7.5, 2H), 2.60 (s, 3H), 2.49 (s, 3H), 1.55 (t, J=7.5, 3H). ^{13}C NMR (500 MHz, DMSO-d_6) δ ppm: 159.61, 155.64, 152.78, 146.76, 138.09, 136.13, 135.39, 131.59, 131.49, 110.82, 45.76, 22.38, 20.71, 14.55.

I-FI (10-ethyl-9-iodo-3,7,8-trimethylbenzo[g]pteridine-2,4(3H,10H)-dione) (7) – Compound **6** (3 g, 7.6 mmol) was partially dissolved in 50 ml of dry DMF, then K_2CO_3 (5.3 g, 38 mmol) and iodomethane (2.4 ml, 5.4 g, 38 mmol) were added. The mixture was stirred at room temperature for three days. Brine (~100 ml) was added to the solution and the mixture was extracted with dichloromethane. Crude product was purified by flash chromatography (acetone:DCM – 1:2) to give 2.6 g (6.3 mmol, 83%) of I-FI as an orange solid. MALDI MS, m/z found: 410.14 [410.02 calculated for $\text{C}_{15}\text{H}_{15}\text{IN}_4\text{O}_2$]. ^1H NMR (500 MHz, DMSO-d_6) δ ppm: 7.99 (s, 1H), 4.87 (q, J=7.5, 2H), 3.27 (s, 3H), 2.61 (s, 3H), 1.55 (t, J=7.5, 3H). ^{13}C NMR (500MHz, DMSO-d_6) δ ppm: 159.85, 155.62, 151.72, 147.41, 137.68, 136.69, 136.03, 132.02, 131.89, 111.20, 45.92, 28.36, 22.86, 21.16, 15.01.

Femtosecond Transient Absorption (fs TA) Experiments. The laser system for the fs TA measurements was described previously.²⁴ Briefly, the 800 nm laser pulses were produced at a 1

1
2
3 kHz repetition rate (fwhm = 110 fs) by a mode-locked Ti:sapphire laser (Hurricane, Spectra-
4 Physics). The output from the Hurricane was split into pump (85 %) and probe (10 %) beams.
5
6 The pump beam (800 nm) was sent into an optical parametric amplifier (OPA-400, Spectra
7 Physics) to obtain the 480 nm pump pulses ($E < 1\mu\text{J}/\text{pulse}$). The probe beam was focused into a
8 horizontally moving CaF_2 crystal for white light continuum generation between 350 and 800 nm.
9
10 The relative polarization between the pump and the probe beams was set at the magic angle
11 (54.7°). The pump and probe beams were overlapped in the sample. The flow cell (Starna Cell
12 Inc. 45-Q-2, 0.9 mL volume with 2 mm path length), pumped by a Fluid Metering RHSY Lab
13 pump (Scientific Support Inc.), was used to prevent photodegradation of the sample. After
14 passing through the cell, the continuum was coupled into an optical fiber and input into a CCD
15 spectrograph (Ocean Optics, S2000). The data acquisition was achieved using in-house
16 LabVIEW (National Instruments) software routines. The group velocity dispersion of the
17 probing pulse was determined using nonresonant optical Kerr effect (OKE) measurements.
18
19 Sample solutions were prepared at a concentration needed to have absorbance of $A \sim 0.6-1.0$ at
20 the excitation wavelength.
21
22
23
24
25
26
27
28
29
30
31
32
33
34
35
36
37

38 **Nanosecond Transient Absorption (ns TA) Experiments.** The nanosecond laser flash
39 photolysis experimental setup utilized for the measurements in this paper is described in detail
40 elsewhere.²⁵ Briefly, a Nd:YAG laser (Spectra Physics LAB-150-10) was used as the excitation
41 light source with an excitation wavelength of 355 nm. The probe light was supplied by a 150 W
42 xenon arc lamp (Applied Photophysics) used in pulsed mode (0.5 ms in duration) with a 1 Hz
43 repetition rate. Transient absorption spectra were recorded using a Roper ICCD-Max 512T
44 digital intensified CCD camera with up to 2 ns temporal resolution. The single wavelength
45 kinetic measurements were recorded using a PMT connected to an oscilloscope (Tektronix TDS
46
47
48
49
50
51
52
53
54
55
56
57
58
59
60

1
2
3 680C 5Gs/s 1 GHz), which was connected to a computer that runs a custom LabView control
4
5 and acquisition program. Sample solutions were prepared at a concentration needed to have
6
7 absorbance of $A \sim 0.5-0.8$ at the excitation wavelength (355 nm). Solutions were placed in a
8
9 quartz cuvette and deoxygenated prior to ns TA experiments by purging with argon.
10
11

12 **Photocatalysis.** A 10 ml vial was charged with the catalyst (1-10 mol%), thiourea (15 mol%, if
13
14 needed) and 3 ml of solvent. The resulting mixture was stirred in the dark until all reagents
15
16 dissolved. Then BnOH (1 eq.) was added and the vial was placed under 12 W LED lamp ($\lambda=440$
17
18 nm). Reaction mixture was stirred for the required time while being monitored by TLC and ^1H
19
20 NMR methods. The supporting information contains the representative NMR spectra (Figures S1
21
22 and S2).
23
24
25
26

27 Example (Table 1. Entry 13): A 10 ml vial was charged with I-F1 (11 mg, 27 μmol), thiourea (31
28
29 mg, 0.41 mmol) and 3 ml of 5% DMSO- d_6 in ACN- d_3 . The mixture was stirred in the dark for 5
30
31 min. Then BnOH (292 mg, 0.28 ml, 2.7 mmol) was added and the vial was placed under 12 W
32
33 LED lamp ($\lambda = 440$ nm). Reaction mixture was stirred for 5 h until full conversion of the starting
34
35 alcohol has been detected. 50 μl of the mixture was diluted up to 0.5 ml and analyzed by ^1H
36
37 NMR to show 98% yield of benzaldehyde (1,3,5-trimethoxybenzene as a standard).
38
39
40

41 **Photostability test.** Oven dried vial was charged with solution of BnOH in 5% DMSO- d_6 in
42
43 CD $_3$ CN (4.7×10^{-3} M, 3 mL), standard, magnetic stirrer bar and thiourea (15 mol%). Then, the
44
45 catalyst (10 mol%) was added and the mixture was stirred in the dark until all reagents were
46
47 dissolved. The vial was placed under LED (440 nm, 12W) and the mixture was stirred under
48
49 light. Reactions were monitored by TLC. Once reaction was complete (155 minutes for F1 and 90
50
51 minutes for I-F1), the product yield was determined using NMR (1,3,5 trimethoxybenzene was
52
53 used as an internal standard). Then, another portion of neat alcohol was added to the mixture and
54
55
56
57
58
59
60

1
2
3 the procedure was repeated for additional cycle. For every additional cycle, the amount of BnOH
4
5 to be added was calculated based on NMR yields to match the initial concentration of 4.7 mmol.
6
7
8

9 10 **Results and Discussions**

11
12
13
14
15 The UV/Vis absorption spectra of Fl and I-Fl (Figure 1a) are similar, with two absorption bands
16
17 at approximately 350 and 450 nm arising due to π,π^* electronic transitions.²² The spectral
18
19 similarity indicates that Fl and I-Fl have almost equal capacity to drive useful photochemical
20
21 transformations using the energy of blue photons. The standard reduction potentials for Fl and I-
22
23 Fl were obtained using cyclic voltammetry (Figure 1b). Both model compounds exhibit two
24
25 reduction peaks associated with the formation of the semiquinone and hydroquinone forms of the
26
27 flavin.²² The I-Fl reduces at a more positive potential, indicating that it is a better electron
28
29 acceptor. Assuming that the triplet excited state energies of Fl and I-Fl are the same, this implies
30
31 that the driving force for the photoinduced electron transfer from T_1 state of I-Fl to the substrate
32
33 is by 0.15 eV larger than the corresponding driving force for Fl.
34
35
36
37
38
39
40
41
42
43
44
45
46
47
48
49
50
51
52
53
54
55
56
57
58
59
60

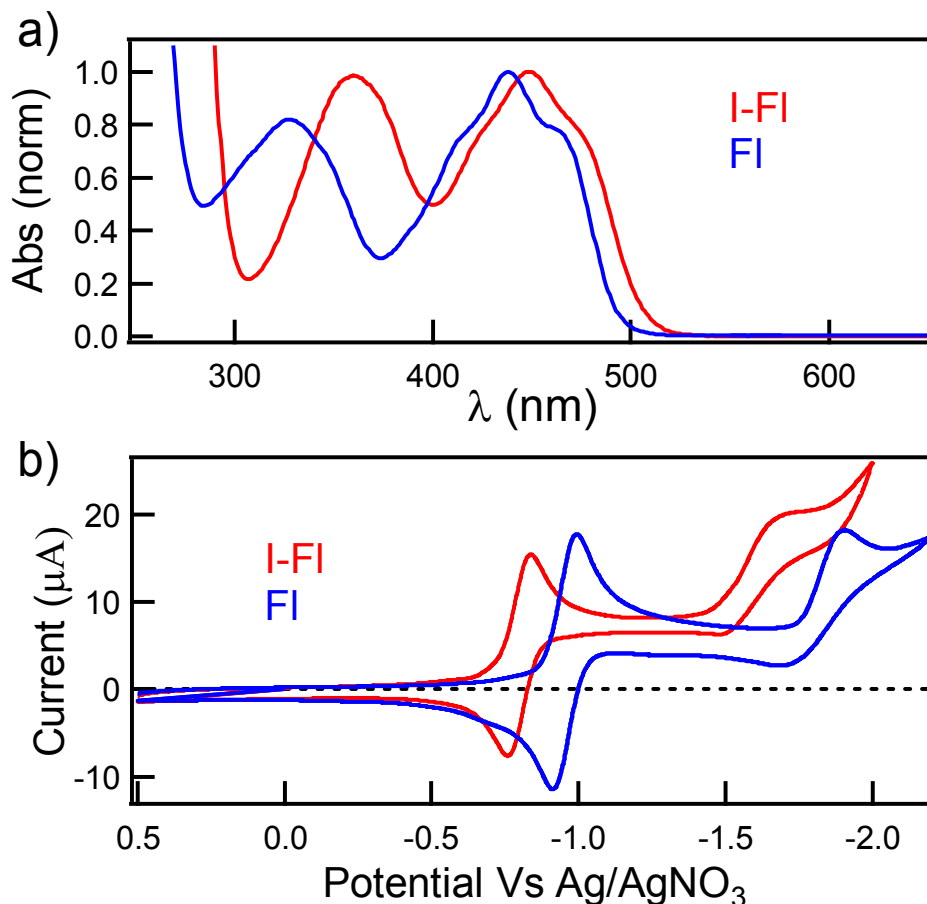


Figure 1. a) Absorption spectra of FI (blue) and I-FI (red) in acetonitrile; (b) cyclic voltammograms of FI (blue) and I-FI (red) in 0.1 M TBAP in acetonitrile (Pt working electrode, 0.1 V/s scan rate). The first reduction potentials are at -0.95 V (FI) at -0.85 V (I-FI) vs. Ag/AgNO₃.

Femtosecond pump-probe experiments were performed to evaluate the ISC rates in model flavins. The transient spectra collected at early times are assigned to the $^1\pi,\pi^*$ states of FI and I-FI (Figure 2a), and consist of the ground state bleach (400-500 nm), stimulated emission (500-700 nm) and excited-state absorption (350-400 nm and ~500 nm) bands. The lifetimes of these $^1\pi,\pi^*$ states are significantly different in the two model compounds: in the case of FI, the $^1\pi,\pi^*$

state decays within several nanoseconds to form the $^3\pi,\pi^*$ state,²² while the spin inversion occurs with a lifetime of only 87 ps for I-FI (Figure 2b). The formation of the $^3\pi,\pi^*$ state of I-FI is observed as growths of absorption bands at 400 nm and in the 500-700 nm range. The significantly faster ISC rate and the absence of ground state bleach recovery in the case of I-FI demonstrates that the incorporation of iodine provides an efficient route towards increased triplet state quantum yields in flavin derivatives.

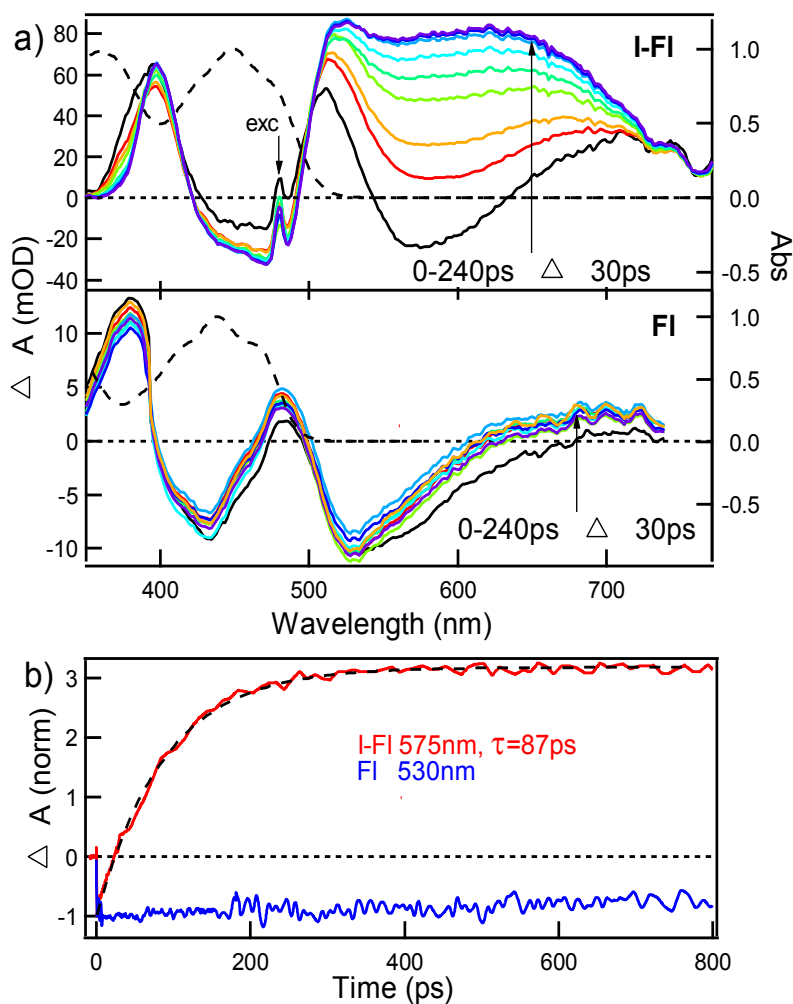


Figure 2. (a) Transient absorption difference spectra of I-FI (upper panel) and FI (lower panel) in acetonitrile (ACN) collected 0-240 ps after the 480 nm excitation pulse. The ground state absorption spectra of FI and I-FI are presented as dashed curves for comparison; (b) Kinetic

1
2
3 profiles for I-Fl, probed at 575 nm (red) with exponential fit (dashed), and Fl, probed at 530 nm
4
5 (blue).
6
7

8
9 The lifetimes of the triplet excited states in Fl and I-Fl were evaluated using nanosecond
10
11 transient absorption spectroscopy (Figure 3). The $^3\pi,\pi^*$ states of Fl and I-Fl exhibit broad
12
13 absorption features that cover the entire visible range (Figure 3a). Both triplets decay on the
14
15 microsecond timescale, as can be observed from the kinetic traces probed at 600 nm (Figure 3b).
16
17

18 The triplet excited lifetime of I-Fl is somewhat shorter (5.8 μs) than the lifetime of the
19
20 corresponding triplet in Fl (12.6 μs). Even though the kinetic traces obtained in Figure 3b were
21
22 obtained using the lowest possible power of the pump beam, it is possible that the lifetimes are
23
24 affected by the bimolecular annihilation processes.²⁶ The shortening of the triplet excited-state
25
26 lifetime in I-Fl is consistent with the heavy atom effect caused by the iodo-substituent: the spin-
27
28 orbit interaction in I-Fl causes not only an increase in the rate of $S_1 \rightarrow T_1$ intersystem crossing
29
30 (Figure 2b), but also leads to increased rate of the $T_1 \rightarrow S_0$ relaxation pathway (Figure 3b).
31
32

33
34 Importantly, this heavy-atom effect is much more pronounced in accelerating the $S_1 \rightarrow T_1$ process
35
36 (ISC rate in I-Fl is ~ 100 times higher than in Fl, Figure 2b) than in accelerating the $T_1 \rightarrow S_0$
37
38 relaxation (rate is only ~ 2 times faster, Figure 3b). Such situation is ideal for promoting the
39
40 photocatalytic processes using triplet excited state of flavin, where one needs high triplet
41
42 quantum yields (which is assured with fast ISC rates) and long triplet excited-state lifetimes, thus
43
44 providing sufficient time for the photochemical event to take place.
45
46
47
48
49
50
51
52
53
54
55
56
57
58
59
60

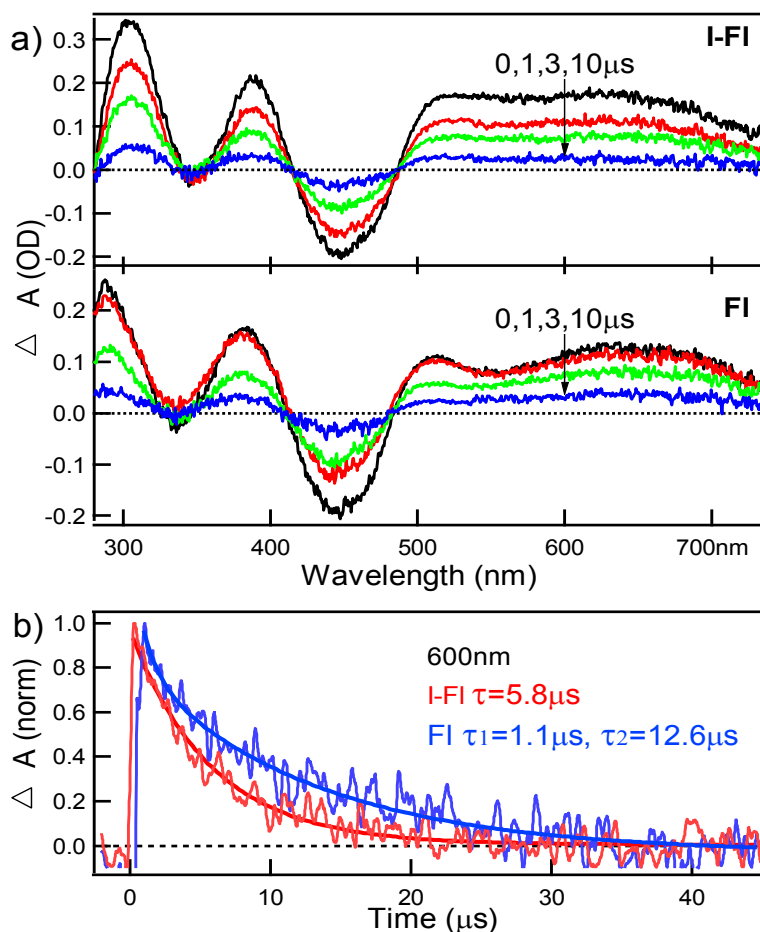
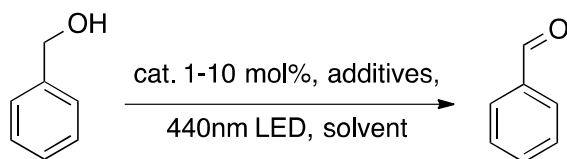


Figure 3. (a) Transient absorption difference spectra of I-FI (upper panel) and FI (lower panel) in acetonitrile (ACN) collected from 0 to 10 μs after the 355 nm excitation pulse; (b) Kinetic profiles for I-FI (red) and FI (blue) probed at 600 nm.

The photocatalytic efficiency of I-FI was evaluated using the oxidation of benzyl alcohol as a model reaction (Scheme 3). The catalysis was evaluated in three solvent mixtures: DMSO/ACN, DMSO/H₂O and ACN/H₂O (Table 1). The product yields were highest in the ACN/H₂O solvent mixture (for example, compare entries 2, 4 and 6), which is consistent with the previous reports showing that the higher polarity solvents more efficiently stabilize the radical ions formed after the photoinduced electron transfer.¹⁶ The addition of thiourea as an electron mediator¹⁰

1
2
3 significantly increases the benzaldehyde yield (for example, compare entries 2 and 8). In
4
5 addition, the 10 mol% catalyst loading gives higher benzaldehyde yields (entry 8) than the 1
6
7 mol% loading (entry 11). Importantly, the comparison of Fl and I-Fl photocatalysis revealed that
8
9 I-Fl provided consistently higher benzaldehyde yields. For example, entries 7 and 8 report two
10
11 reactions in which all experimental conditions were identical, except that different catalysts were
12
13 used. While the I-Fl catalyst provided a 100% yield of benzaldehyde, the yield in the presence of
14
15 Fl was only 72%. These results are consistent with the previous report¹⁷ showing that the
16
17 efficient catalysis occurs from the triplet excited-state of flavin, while the singlet excited state
18
19 leads to undesired charge recombination process. Since the iodine in I-Fl provides higher triplet
20
21 quantum yield and lower singlet excited-state lifetime, the photocatalysis is more efficient for I-
22
23 Fl.
24
25
26
27
28
29

30 **Scheme 3.** Organocatalytic photooxidation of benzyl alcohol.



43 **Table 1.** Catalytic Photooxidation with Flavins.

44
45
46
47
48
49
50
51
52
53
54
55
56
57
58
59
60

Entry	Catalyst, (mol%)	Solvent	Time, h	Yield, ^a %
1	Fl (10)	5% DMSO in ACN	1.5	31
2	I-Fl (10)	5% DMSO in ACN	1.5	42
3	Fl (10)	5% DMSO	1.5	41

		in H ₂ O		
4	I-F1 (10)	5% DMSO in H ₂ O	1.5	54
5	F1 (10)	ACN:H ₂ O (1:2)	1.5	77
6	I-F1 (10)	ACN:H ₂ O (1:2)	1.5	89
7 ^b	F1 (10)	5% DMSO in ACN	1.5	72
8 ^b	I-F1 (10)	5% DMSO in ACN	1.5	>95
9 ^b	F1 (10)	5% DMSO in ACN	2.5	>95
10 ^b	F1 (1)	5% DMSO in ACN	12	48
11 ^b	I-F1 (1)	5% DMSO in ACN	12	54
12 ^{b,c}	F1 (1)	5% DMSO in ACN	5	21
13 ^{b,c}	I-F1 (1)	5% DMSO in ACN	5	>95

Conditions: benzyl alcohol 4.5×10^{-3} M a) NMR yields, 1,3,5-trimethoxybenzene as a standard, b) thiourea 15 mol%, c) 0.9 M of BnOH

Furthermore, the use of I-F1 as a photocatalyst allows the use of higher concentrations of the benzyl-alcohol substrate. To avoid the unwanted charge recombination that occurs from the singlet excited state pathway, the catalysis by flavins is optimal when lower concentrations of

1
2
3 reactant are used (highest yields were obtained at 25 mM substrate concentration).¹⁷ Similar
4
5 behavior was observed in this work: when benzyl alcohol concentration was increased from 4.5
6
7 mM to 0.9 M, the product yield in the presence of Fl as a catalyst decreased from 48 to 21%
8
9 (entries 10 and 12). The opposite results were obtained when I-Fl was used as a catalyst (entries
10
11 11 and 13), where almost quantitative conversion occurred at 0.9 M substrate concentration. The
12
13 improved catalytic efficiency of I-Fl at high substrate concentration is expected to facilitate the
14
15 scale-up of the flavin-based photooxidation reactions.
16
17

18
19 The photocatalytic performance of I-Fl was compared to that of Fl by evaluating the time it takes
20
21 to bring the BnOH oxidation to completion. In the case of Fl, the reaction took 120 minutes,
22
23 while I-Fl photocatalysis required only 90 minutes under identical experimental conditions (entry
24
25 1, Figure 4). These results indicate that the quantum yield for I-Fl catalysis is higher than for Fl,
26
27 and are consistent with the higher photoreactivity of the triplet excited state. However,
28
29 subsequent addition of BnOH to the reaction mixture (entries 2-4, Figure 4) led to a decrease in
30
31 oxidation yields for both Fl and I-Fl, indicating that the model flavin catalysts undergo
32
33 photodecomposition. In the case of I-Fl, the photodecomposition was more pronounced, as
34
35 evidenced by a more drastic decrease in the product yields. It appears that the triplet excited state
36
37 in I-Fl is responsible for the unwanted photochemical reaction that causes the catalyst
38
39 decomposition.
40
41
42
43
44
45
46
47
48
49
50
51
52
53
54
55
56
57
58
59
60

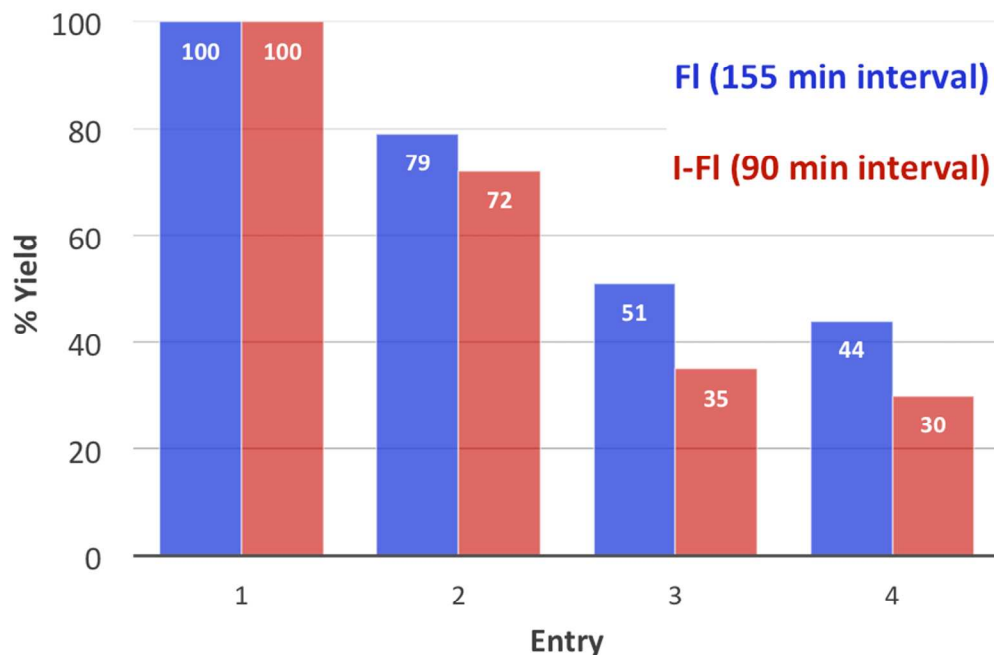
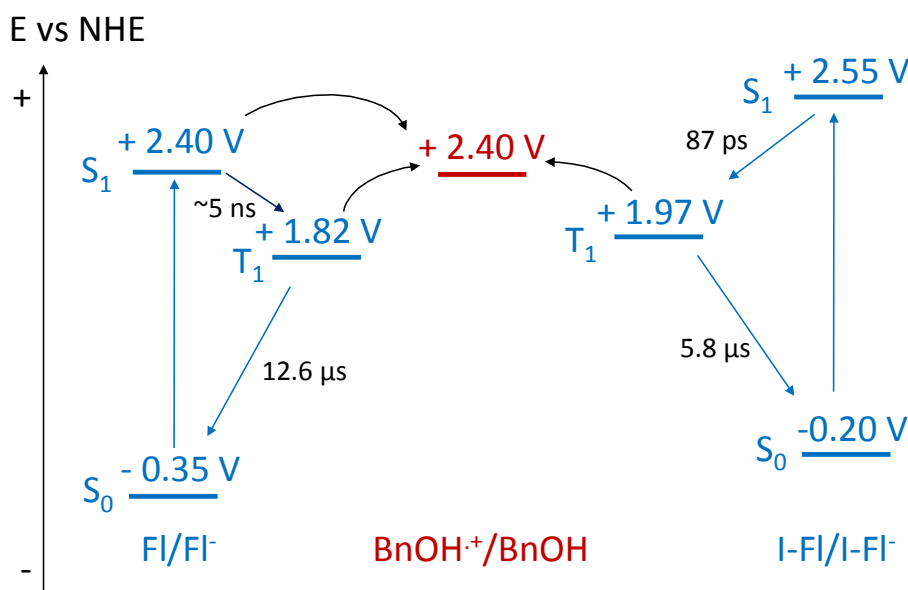


Figure 4. The % yields of benzaldehyde formed using FI (blue) or I-FI (red) as a photocatalyst.

The BnOH oxidation was performed until all alcohol was converted to aldehyde (which took 155 minutes for FI and 90 minutes for I-FI). Then, a new portion of BnOH was added and the procedure was repeated in the same time interval. The reactions were performed in 5% DMSO-d₆ in CD₃CN and in the presence of 15 mol% urea.

To evaluate the energetics for the photoinduced charge transfer from excited FI and I-FI, a diagram showing the reduction potentials of excited flavin models is shown in Scheme 4. The reported potentials are only estimates rather than the exact values, because the standard reduction potential of benzyl alcohol radical cation (BnOH^{•+}) is not known (instead, anodic peak potential for BnOH oxidation was used²⁷) and because the reduction potentials for the flavin models in their T₁ state were obtained under assumption that their triplet energies are the same as that of riboflavin.²⁸ Despite these possible sources of error, it appears that the photoinduced electron

transfer is thermodynamically favorable only for the flavins in their singlet excited state. Surprisingly, the reduction potentials of Fl and I-Fl in their triplet states are significantly below the oxidation potential of BnOH, making it unlikely that the photoinduced electron transfer from T_1 states of flavins to BnOH is taking place. Based on these thermodynamic arguments, we postulate that the photooxidation of BnOH proceeds by a hydrogen atom transfer mechanism. However, further time-resolved experiments are needed to provide more insights into this process.



Scheme 4. Diagram showing the standard reduction potentials of relevant species. The standard reduction potentials of Fl and I-Fl in their ground states were obtained from the cyclic voltammograms in Figure 1b. The corresponding potentials in the S_1 states were obtained using the energies of the lowest absorption bands shown in Figure 1a. The potentials in the T_1 states were obtained assuming the triplet energy of riboflavin (2.17 eV).²⁸ For the oxidation potential of BnOH, the anodic peak potential value for a chemically irreversible oxidation was used.²⁷

Conclusion

1
2
3
4
5
6 In conclusion, the iodo-substituted flavin was synthesized and shown to exhibit higher rate of
7 triplet formation and improved photocatalytic efficiency. These results verify that the triplet
8 excited-state of flavin plays an important role in photocatalytic oxidations of organic substrates.
9
10 Our findings are expected to contribute to the current research efforts in the area of
11 photocatalytic organic synthesis.²⁹⁻³¹ Furthermore, the iodo-flavin analog reported here will
12 likely find applications in biological sciences, as an artificial cofactor for photoactive
13 flavoproteins.³²⁻³⁴
14
15
16
17
18
19
20
21
22
23

24 ASSOCIATED CONTENT

25 26 27 **Supporting Information.**

28
29
30
31 The Supporting Information is available free of charge via the Internet at <http://pubs.acs.org>.

32
33
34
35 Photocatalysis data.

36 37 38 AUTHOR INFORMATION

39 40 **Corresponding Author**

41
42
43 *kglusac@bgsu.edu

44
45
46 The authors declare no competing financial interest.

47 48 49 **Funding Sources**

50
51 We are grateful to the National Science Foundation (CHE-1055397 to K.D.G. and DMR-
52 1212842 to C.M.H.) for funding this work.
53
54
55
56
57
58
59
60

REFERENCES

- 1
2
3
4
5
6
7
8
9
10
11 (1) Huijbers, M. M. E.; Montersino, S.; Westphal, A. H.; Tischler, D.; van Berkel, W. J. H.
12 Flavin Dependant Monooxygenases. *Arch Biochem Biophys* **2014**, *544*, 2.
13
14
15
16 (2) Mansoorabadi, S. O.; Thibodeaux, C. J.; Liu, H. W. The Diverse Roles of Flavin
17 Coenzymess - Nature's Most Versatile Thespians. *J Org Chem* **2007**, *72*, 6329.
18
19
20
21
22 (3) Gadda, G. Hydride Transfer Made Easy in the Reaction of Alcohol Oxidation Catalyzed
23 by Flavin-dependent Oxidases. *Biochemistry* **2008**, *47*, 13745.
24
25
26
27
28 (4) Schaefer-Ramadan, S.; Gannon, S. A.; Thorpe, C. Human Augmenter of Liver
29 Regeneration: Probing the Catalytic Mechanism of a Flavin-Dependent Sulfhydryl Oxidase.
30 *Biochemistry* **2013**, *52*, 8323.
31
32
33
34
35
36 (5) Fagan, R. L.; Palfey, B. A. In *Comprehensive Natural Products II*; Liu, H.-W., Mander,
37 L., Eds.; Elsevier: Oxford, 2010, p 37.
38
39
40
41
42 (6) Cashman, J. R.; Motika, M. S. In *Comprehensive Toxicology (Second Edition)*;
43 McQueen, C. A., Ed.; Elsevier: Oxford, 2010, p 77.
44
45
46
47 (7) Iida, H.; Imada, Y.; Murahashi, S. I. Biomimetic Flavin-Catalysed Reactions for Organic
48 Synthesis. *Org Biomol Chem* **2015**.
49
50
51
52
53 (8) Lechner, R.; Kümmel, S.; König, B. Visible Light Flavin Photo-Oxidation of
54 Methylbenzenes, Styrenes and Phenylacetic Acids. *Photochem Photobiol Sci* **2010**, *9*, 1367.
55
56
57
58
59
60

- 1
2
3 (9) Schmaderer, H.; Hilgers, P.; Lechner, R.; König, B. Photooxidation of Benzyl Alcohols
4 with Immobilized Flavins. *Adv Synth Catal* **2009**, *351*, 163.
5
6
7
8
9 (10) Svoboda, J.; Schmaderer, H.; König, B. Thiourea-Enhanced Flavin Photooxidation of
10 Benzyl Alcohol. *Chem-Eur J* **2008**, *14*, 1854.
11
12
13
14 (11) Fukuzumi, S.; Kuroda, S. Photooxidation of Benzyl Alcohol Derivatives By Oxygen,
15 Catalyzed By Protonated Flavin Analogues. *Res Chem Intermediat* **1999**, *25*, 789.
16
17
18
19
20 (12) Fukuzumi, S.; Yasui, K.; Suenobu, T.; Ohkubo, K.; Fujitsuka, M.; Ito, O. Efficient
21 Catalysis of Rare-Earth Metal Ions in Photoinduced Electron-Transfer Oxidation of Benzyl
22 Alcohols by a Flavin Analogue. *J Phys Chem A* **2001**, *105*, 10501.
23
24
25
26
27
28 (13) Tong, W.; Ye, H. P.; Zhu, H. H.; D'Souza, V. T. Photooxidation of Substituted Benzyl
29 Alcohol by Riboflavin. *Theochem-J Mol Struc* **1995**, *333*, 19.
30
31
32
33
34 (14) Fukuzumi, S.; Tanii, K.; Tanaka, T. Protonated Pteridine and Flavin Analogues acting as
35 Efficient and Substrate-selective Photocatalysts in the Oxidation of Benzyl Alcohol Derivatives
36 by Oxygen. *J Chem Soc Chem Comm* **1989**, 816.
37
38
39
40
41
42 (15) Haas, W.; Hemmerich, P. Flavin-Dependent Substrate Photo-oxidation as a Chemical
43 Model of Dehydrogenase Action. *Biochem J* **1979**, *181*, 95.
44
45
46
47
48 (16) Feldmeier, C.; Bartling, H.; Magerl, K.; Gschwind, R. M. LED-Illuminated NMR Studies
49 of Flavin-Catalyzed Photooxidations Reveal Solvent Control of the Electron-Transfer
50 Mechanism. *Angew Chem Int Ed* **2015**, *54*, 1347.
51
52
53
54
55
56
57
58
59
60

- 1
2
3 (17) Megerle, U.; Wenninger, M.; Kutta, R. J.; Lechner, R.; König, B.; Dick, B.; Riedle, E.
4
5 Unraveling the Flavin-catalyzed Photooxidation of Benzylic Alcohol with Transient Absorption
6
7 Spectroscopy from Sub-pico- to Microseconds. *Phys Chem Chem Phys* **2011**, *13*, 8869.
8
9
10
11 (18) Gelalcha, F. G. Heterocyclic Hydroperoxides in Selective Oxidations. *Chem Rev* **2007**,
12
13 *107*, 3338.
14
15
16
17 (19) Massey, V. Activation of Molecular Oxygen by Flavins and Flavoprotein. *J Biol Chem*
18
19 **1994**, *269*, 22459.
20
21
22
23 (20) Frederick, R. E.; Mayfield, J. A.; DuBois, J. L. Regulated O₂ Activation in Flavin-
24
25 Dependent Monooxygenases. *J Am Chem Soc* **2011**, *133*, 12338.
26
27
28
29 (21) Koziar, J. C.; Cowan, D. O. Photochemical Heavy-atom Effects. *Acc Chem Res* **1978**, *11*,
30
31 334.
32
33
34 (22) Sichula, V.; Kucheryavy, P.; Khatmullin, R.; Hu, Y.; Mirzakulova, E.; Vyas, S.; Manzer,
35
36 S. F.; Hadad, C. M.; Glusac, K. D. Electronic Properties of N(5)-Ethyl Flavinium Ion. *J Phys*
37
38 *Chem A* **2010**, *114*, 12138.
39
40
41
42 (23) Mirzakulova, E.; Khatmullin, R.; Walpita, J.; Corrigan, T.; Vargas-Barbosa, N. M.; Vyas,
43
44 S.; Oottikkal, S.; Manzer, S. F.; Hadad, C. M.; Glusac, K. D. Electrode-assisted Catalytic Water
45
46 Oxidation by a Flavin Derivative. *Nat Chem* **2012**, *4*, 794.
47
48
49
50 (24) Li, G.; Glusac, K. D. Light-Triggered Proton and Electron Transfer in Flavin Cofactors. *J*
51
52 *Phys Chem A* **2008**, *112*, 4573.
53
54
55
56
57
58
59
60

- 1
2
3 (25) Martin, C. B.; Tsao, M. L.; Hadad, C. M.; Platz, M. S. The Reaction of Triplet Flavin
4 with Indole. A Study of the Cascade of Reactive Intermediates Using Density Functional Theory
5 and Time Resolved Infrared Spectroscopy. *J Am Chem Soc* **2002**, *124*, 7226.
6
7
8
9
10
11 (26) Yoshimura, A.; Ohno, T. Quenching of Excited Triplet Lumiflavin by Lumiflavin
12 Radicals Formed in its T-T Reaction. *Photochem Photobiol* **1991**, *53*, 175.
13
14
15
16
17 (27) Higashimoto, S.; Suetsugu, N.; Azuma, M.; Ohue, H.; Sakata, Y. Efficient and Selective
18 Oxidation of Benzylic Alcohol by O₂ into Corresponding Aldehydes on a TiO₂ Photocatalyst
19 Under Visible Light Irradiation: Effect of Phenyl-ring Substitution on the Photocatalytic
20 Activity. *J Catal* **2010**, *274*, 76.
21
22
23
24
25
26
27 (28) S. L. Murov, I. C., G. L. Hug *Handbook of Photochemistry*; 2nd edn. ed. New York,
28 1993.
29
30
31
32
33 (29) Prier, C. K.; Rankic, D. A.; MacMillan, D. W. Visible Light Photoredox Catalysis with
34 Transition Metal Complexes: Applications in Organic Synthesis. *Chem Rev* **2013**, *113*, 5322.
35
36
37
38
39 (30) Yoon, T. P.; Ischay, M. A.; Du, J. Visible Light Photocatalysis as a Greener Approach to
40 Photochemical Synthesis. *Nat Chem* **2010**, *2*, 527.
41
42
43
44
45 (31) Hamilton, D. S.; Nicewicz, D. A. Direct Catalytic Anti-Markovnikov Hydroetherification
46 of Alkenols. *J Am Chem Soc* **2012**, *134*, 18577.
47
48
49
50
51 (32) Brust, R.; Lukacs, A.; Haigney, A.; Addison, K.; Gil, A.; Towrie, M.; Clark, I. P.;
52 Greetham, G. M.; Tonge, P. J.; Meech, S. R. Proteins in Action: Femtosecond to Millisecond
53 Structural Dynamics of a Photoactive Flavoprotein. *J Am Chem Soc* **2013**, *135*, 16168.
54
55
56
57
58
59
60

(33) Sancar, A. Cryptochrome: The Second Photoactive Pigment in the Eye and Its Role in Circadian Photoreception. *Ann Rev Biochem* **2000**, *69*, 31.

(34) Zhong, D.; Zewail, A. H. Femtosecond Dynamics of Flavoproteins: Charge Separation and Recombination in Riboflavine (Vitamin B₂)-Binding Protein and in Glucose Oxidase Enzyme. *Proc Natl Acad Sci* **2001**, *98*, 11867.

Table of Contents Artwork

